Thermal Conductivity of Gaseous Trifluoroiodomethane (CF_3I)

Y. Y. Duan, L. Q. Sun, L. Shi, M. S. Zhu,* and L. Z. Han

Thermal Engineering Department, Tsinghua University, Beijing 100084, People's Republic of China

The thermal conductivity of gaseous trifluoroiodomethane (CF_3I) is reported over the temperature range −6.50 °C to 63.55 °C at pressures up to 1000 kPa with an uncertainty of 3% using a transient hot-wire instrument employing two anodized tantalum wires as the heat source. The results were correlated as a function of temperature and density. The values for the thermal conductivity of the dilute gas and the saturated vapor are obtained by extrapolation.

Introduction

The traditional refrigerant CFC-12 is widely used in numerous applications. Alternatives of CFC-12 must be developed that are environmentally acceptable and can be used in high-capacity, high-efficiency applications. So far, many CFC alternatives have been developed. HFC-134a has been widely used as a replacement for CFC-12, especially in the United States, Japan, the United Kingdom, and France. But HFC-134a requires physical retrofitting of equipment and does not mix with conventional lubricants. It also has higher global warming potential (GWP) value. Even though they are flammable, hydrocarbons are considered to be another promising alternative, especially in Germany. CF_3I has been found to be nonozone depleting, miscible with mineral oil, and compatible with refrigeration system materials. It also has an extremely low GWP value and very low acute toxicity. Therefore, it is also being considered as a promising alternative, especially as a component in mixtures, to replace CFC-12 (Lankford and Nimitz, 1993; Zhao et al., 1995). However, no reliable data for the thermal conductivity of CF_3I has been published in recent years. Therefore, research on the thermal conductivity of CF_3I is of great interest. This paper reports experimental data for the thermal conductivity of gaseous CF_3I in the temperature range from −6.5 to 63.55 °C at pressures up to 1000 kPa with an uncertainty of 3%.

Working Equation

The theoretical basis of the transient hot-wire technique for gas thermal conductivity measurements has been given in detail elsewhere (Healy et al., 1976). According to the theory, the thermal conductivity, λ, of the fluid can be obtained with the following equations

$$\Delta T_{\mathrm{id}} = \Delta T_{\mathrm{w}} + \sum \delta T_i = \frac{q}{4\pi\lambda(T_{\mathrm{r}},\rho_{\mathrm{r}})} \ln\frac{4k\tau}{a^2 C} \qquad (1)$$

and

$$T_{\mathrm{r}} = T_0 + {}^1/_2(\Delta T_1 + \Delta T_2) \qquad (2)$$

where T_0 is the equilibrium temperature of the fluid before heating, T_{r} is the reference temperature, ρ_{r} is the density of the fluid at the reference temperature T_{r} and the primary pressure p_0, q is the energy input per unit length of the hot-wire, τ is the time of heating, a is the wire radius, λ is the thermal conductivity of the fluid at temperature T_{r} and pressure p_0, ΔT_{id} is the temperature rise of the hot-wire under the ideal conditions, ΔT_1 and ΔT_2 are the temperature rises of the hot-wire at the initial moment and the final moment respectively, and C is a numerical constant. The symbol k represents the thermal diffusivity of the fluid surrounding the wires. The various correction terms, δT_i, have all been identified (Healy et al., 1976) and are all rendered less than 1% of ΔT_{id} except the correction term induced by the thermophysical properties of the hot-wire, which is rendered less than 3% of ΔT_{id} in the interested time range by the design of the wires and the operation of the instrument. It follows from eq 1 that an essential feature of the correct operation of the instrument is that the measured ΔT_{id} should be a linear function of the logarithm of time, ln τ. Once the temperature rise of the hot-wire is measured as a function of time, τ, the gradient of the linear function of ΔT_{id} versus the logarithm of τ can be used to calculate the thermal conductivity λ.

Instrument

The thermal conductivity instrument was described in detail in a previous work (Sun et al., 1997); a modified apparatus is used in this work. The outer part of the instrument is a pressure vessel made of stainless steel which can withstand the pressure of 6 MPa. The inner part which contains the hot-wires is composed of two compartments formed by machining two identical holes centering on the split diameter of a copper cylinder and parallel to its axis. The half of the cylinder shown in Figure 1 carries the five wire supports and is itself supported by the aluminum ring attached to the outer pressure vessel.

In this instrument, two 25 μm tantalum wires were used as the hot-wires (13.4 cm and 4.1 cm in length). The wires were anodized *in situ* to form a layer of insulating tantalum pentoxide on their surface. All electrical connections to the hot-wires were made of 0.8 mm diameter enamel-insulated wire which extends outside of the pressure vessel. The wires were kept vertical and under constant tension by a copper block attached to the bottom of each wire. The mass of the copper blocks was chosen to keep the tension of the hot-wires at 25% of the yielding tension (Menashe and Wakeham, 1981). The wires were connected very carefully to eliminate contact resistance in the measuring system. The instrument employs two hot-wires to eliminate the errors caused by the finite length by using the short wire to compensate for the long wire (Kestin and Wakeham, 1978).

The wires were calibrated carefully *in situ* to determine the resistance temperature coefficient of the tantalum wire.

* To whom correspondence should be addressed. E-mail: dmc@mail.tsinghua.edu.cn.

S0021-9568(97)00037-X CCC: $14.00

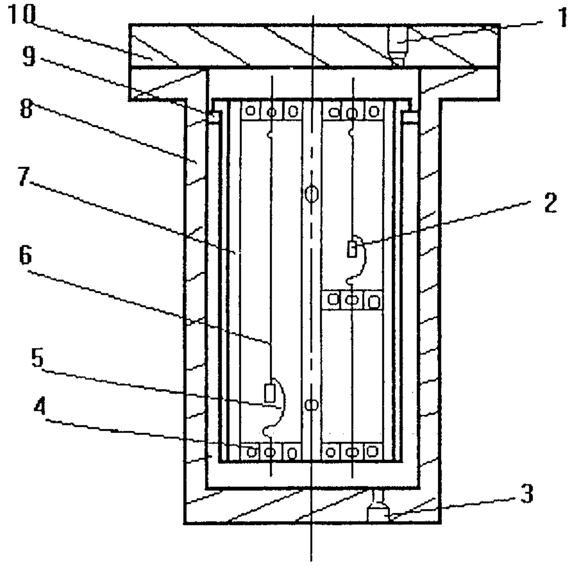

Figure 1. Instrument schematic: 1, holes for wire extension; 2, copper block; 3, tested fluid charging hole; 4, mount for wires; 5, gold strip; 6, tantalum wire; 7, copper compartment; 8, pressure vessel; 9, aluminum ring; 10, flange plate.

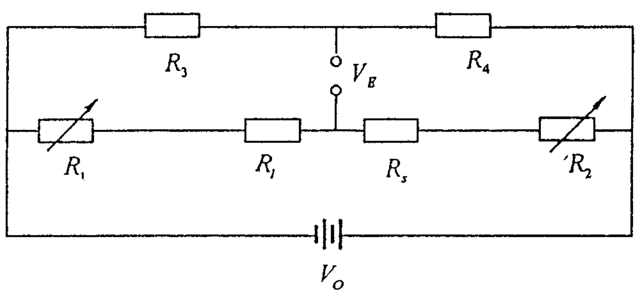

Figure 2. Unbalanced bridge employed in this work.

The tantalum wire resistance, $R(\Omega)$, was represented as a polynomial function of the temperature t, over the temperature range from −10 to 65 °C. A least-squares analysis of the data yielded

$$R(t) = R_0[1 + 3.4155 \times 10^{-3}(t/°C) - 1.29192 \times 10^{-6}(t/°C)^2] \quad (3)$$

where R_0 represents the resistance of the hot-wires at a temperature of 0 °C. The resistance changes and thus the temperatures rise of the wires were measured by an unbalanced bridge as shown in Figure 2. With this bridge, the difference between the resistance of the two wires can be written in the following form as the two wires are identical except for their length.

$$\Delta R = R_l - R_s = \left(\frac{l_l}{l_s} - 1\right)\frac{CR_1 + CR_2 - R_1}{\frac{l_l}{l_s}(1 - C) - C} \quad (4)$$

in which

$$C = \frac{V_E}{V_0} + \frac{R_3}{R_3 + R_4} \quad (5)$$

where R_l is the resistance of the long hot-wire, R_s is the resistance of the short hot-wire, l_l is the length of the long wire, l_s is the length of the short wire, V_0 is the voltage of the power source, V_E is the measured voltage across the bridge measured; R_1 and R_2 are the resistances of two adjustable resistors, and R_3 and R_4 are the resistances of two standard fixed resistors. Resistors R_1 and R_2 were carefully chosen to ensure a uniform energy input, q, into the experiment. The bridge voltage, V_E, was measured with a Hewlett Packard 3852A acquisition unit at a collecting rate of about 30 points per s. The temperature rise of the hot-wires was about 3−4 K in the experiment. The instrument uncertainty was estimated less than 3%.

The pressure-measurement system included a piston-type pressure gauge, a pressure transducer, and an atmosphere pressure gauge. The accuracy of the piston-type pressure gauge was less than 0.005% in the range 0.1 to 6 MPa. A very sensitive diaphragm pressure transducer (405T) separated the sample from an N_2-filled system including the precision piston-type pressure gauge. The accuracy of the transducer was 0.2%, the pressure difference adjustable range was 6 to 38 kPa, the temperature range was 233 to 400 K, and the maximum allowable pressure was 17.8 MPa. The accuracy of the atmospheric pressure gauge was 0.05% over a pressure range of 1 to 160 kPa. The whole pressure measurement system had an uncertainty of ±500 Pa.

The bath temperature could be varied from 223 to 452 K. The temperature instability was less than ±5 mK per 8 h. The overall temperature uncertainty for the bath and temperature-measurement system was less than ±10 mK.

Table 1. Measurements of the Thermal Conductivity of N_2

P/kPa	t/°C	λ_{lit}/mW·m^{-1}·K^{-1}	λ_{exp}/mW·m^{-1}·K^{-1}	$\lambda_{exp} - \lambda_{lit}$/mW·m^{-1}·K^{-1}	$((\lambda_{exp}/\lambda_{lit}) - 1) \times 100$
2058.86	23.43	26.814	26.778	−0.036	−0.134
			26.883	0.069	0.257
1702.44	23.36	26.639	26.648	0.009	0.034
			26.611	−0.028	−0.105
1202.85	23.41	26.392	26.305	−0.087	−0.330
			26.412	0.020	0.076
714.84	23.55	26.167	26.080	−0.087	−0.332
			26.042	−0.125	−0.478
436.00	23.78	26.050	25.905	−0.145	−0.557
			25.831	−0.219	−0.841

Results and Analysis

Before the thermal conductivity of gaseous CF_3I was measured, the thermal conductivity of nitrogen near the isotherm of 23.55 °C was measured and compared with values calculated from an equation recommended in the literature (Stephan et al., 1987). The recommended equation has an accuracy of ±0.8%. The measured nitrogen thermal conductivity is listed in Table 1 along with the deviation from the calculated values. The maximum deviation of the measured nitrogen thermal conductivity is less than 1%, and the root mean square deviation is 0.42%. The mass purity of the used nitrogen sample was 99.95%.

The thermal conductivity of gaseous CF_3I was then measured. The mass purity of the CF_3I sample is 99.95%. Figure 3 shows the pressure range and temperature range of the experimental points. Figure 4 shows the temperature rise ΔT versus the logarithm of time τ for a typical run using nitrogen at a bath temperature of 20 °C and a pressure of 436.00 kPa and a typical run using CF_3I at a bath temperature of 30 °C and a pressure of 139.93 kPa. The solid line is a linear correlation for CF_3I, while the dashed line is a linear correlation for nitrogen. The correlations were determined using a least-squares analysis. There are three parts in the two curves. The first part of each curve is a segment where the thermophysical properties of the hot-wire shows an significant effect and

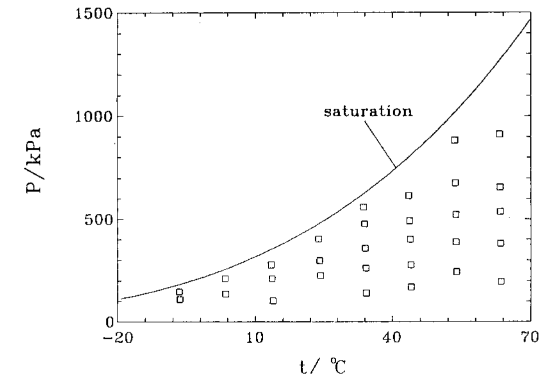

Figure 3. Temperature and pressure ranges for the experimental points.

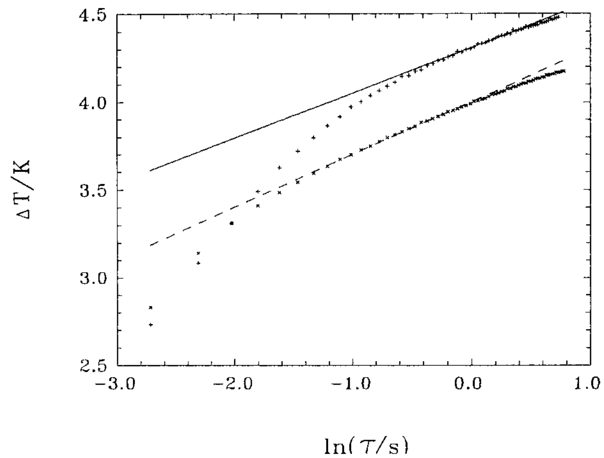

Figure 4. Temperature rise of hot-wire and its linear function versus the logarithm of time for both CF_3I and nitrogen: (—) CF_3I; (- - -) nitrogen.

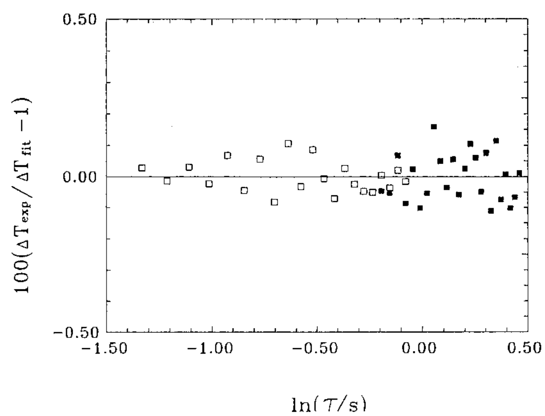

Figure 5. Deviation of temperature rise of hot-wire from the correlated linear function for both CF_3I and nitrogen: (□) nitrogen; (■) CF_3I.

the third part is a segment where natural convection begins to appear and shows a significant effect. The middle part can be described by eqs 1 and 2. Because the thermal conductivity of nitrogen is larger than that of CF_3I at corresponding thermodynamic states, the effect of the hot-wire thermophysical properties on the measurement for nitrogen can be ignored earlier than CF_3I according to the theory of Healy (1976). The relative deviations of the experimentally measured temperature rise from the linear function in Figure 4 are shown in Figure 5 for nitrogen and for CF_3I respectively at the thermodynamic states in Figure 4. No curvature or systematic trend is apparent, and the maximum deviation is less than 0.2%. Similar plots were prepared for all the measurements described

Table 2. Thermal Conductivity for CF_3I

t/°C	p/kPa	ρ_{cal}/kg·m^{-3}	λ/mW·m^{-1}·K^{-1}
−6.60	147.40	13.861	6.624
−6.50	109.56	10.125	6.594
3.40	211.37	19.381	6.998
3.53	136.51	12.126	6.923
13.50	277.63	24.776	7.402
13.65	210.25	18.346	7.286
13.88	103.26	8.719	7.155
23.79	403.76	35.629	8.026
24.01	298.90	25.547	7.831
24.20	225.67	18.892	7.611
33.70	558.50	49.031	8.623
33.94	476.54	40.822	8.423
34.07	357.80	29.698	8.136
34.20	261.25	21.176	7.956
34.33	139.93	11.035	7.721
43.50	615.78	52.193	9.032
43.70	491.57	40.369	8.745
43.82	400.39	32.189	8.512
43.94	276.87	21.674	8.233
44.06	169.43	12.980	8.034
53.43	883.53	76.186	9.876
53.54	677.54	55.482	9.392
53.66	522.99	41.392	9.034
53.70	388.91	29.970	8.767
53.80	243.84	18.294	8.476
63.25	912.58	75.123	10.123
63.30	656.80	51.218	9.704
63.37	537.58	40.984	9.442
63.45	380.88	28.252	9.123
63.55	195.21	14.054	8.745

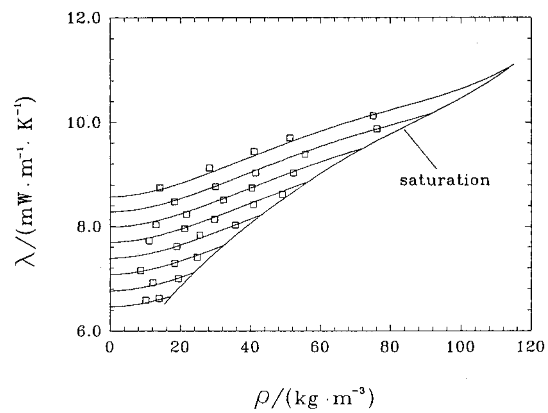

Figure 6. Thermal conductivity of gaseous CF_3I vs density near different isotherms. The temperatures of the isotherms are −6.5 °C, 3.5 °C, 13.6 °C, 24.0 °C, 34.0 °C, 43.8 °C, 53.6 °C, and 63.4 °C, respectively.

in this paper. The lack of any curvature or systematic trend as well as the magnitude of the deviation indicates that no radiation correction is necessary for the temperature range considered (Nieto de Castro et al., 1991).

All of the results are given in Table 2. The thermal conductivity data was fit to the following equation using a least-squares analysis

$$\lambda/\mathrm{mW{\cdot}m^{-1}{\cdot}K^{-1}} = a_0 + a_1(t/°\mathrm{C}) + b_2(\rho/\mathrm{kg{\cdot}m^{-3}})^2 + b_3(\rho/\mathrm{kg{\cdot}m^{-3}})^3 + b_4(\rho/\mathrm{kg{\cdot}m^{-3}})^4 \quad (6)$$

The coefficients were determined to be: $a_0 = 6.661\ 404$, $a_1 = 3.018\ 743 \times 10^{-2}$, $b_2 = 8.299\ 915 \times 10^{-4}$, $b_3 = -1.074\ 127 \times 10^{-5}$, $b_4 = 4.509\ 508 \times 10^{-8}$. The density of CF_3I was calculated by the equation of state provided by Duan et al. (1997). Figure 6 shows the thermal conductivity of CF_3I as a function of density near each isotherm, using the vapor pressure equation provided by Duan et al. (1996). Figure 7 shows the deviations of the experimentally measured CF_3I thermal conductivity from eq 6, where λ_{exp} represents

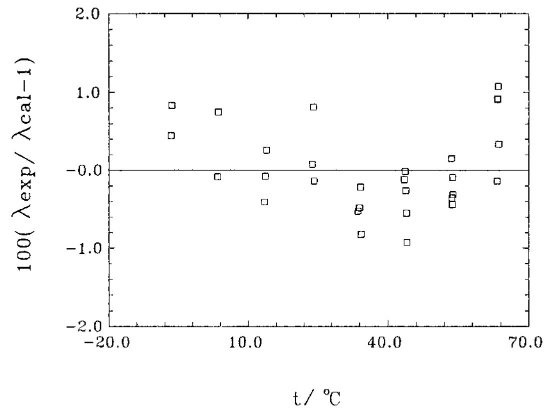

Figure 7. Deviations of the experimental thermal conductivity from eq 6.

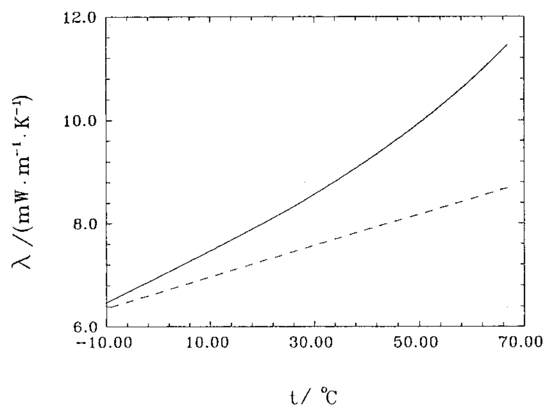

Figure 8. Curvatures of thermal conductivity for the saturation vapor and the ideal gas of CF_3I: (—) curvature for saturation vapor; (- - -) curvature for dilute gas.

the experimental results and λ_{cal} are the values calculated from eq 6. The maximum deviation of the experimental results of from eq 6 is 1.1%. The standard deviation of the experimentally measured data from eq 6 is 0.54%.

Since eq 6 contains no linear density term, the effect of density on the thermal conductivity is strongly reduced close to the dilute gas state (i.e. $\rho \rightarrow 0$). At this state the density effect should vanish according to the kinetic theory of gases. Equation 6 permits determination of the thermal conductivity of both superheated gas and gas at saturation conditions (solid-line curves in Figure 6). For practical calculations, the thermal conductivities for saturation vapor as well as for the dilute gas ($\rho \rightarrow 0$) are of special interest. The thermal conductivity for these two states are plotted as a function of temperature in Figure 8. The results were extrapolated along isotherms since the density range did not extend to two thermodynamic states. However the density range is wide enough for extrapolation, and the errors caused by extrapolation can be ignored. The thermal conductivity for saturated vapor and for dilute gas, indicated by λ'' and λ_0 respectively, are correlated as

$$\lambda''/\mathrm{mW^{-1}\cdot m^{-1}\cdot K^{-1}} = c_0 + c_1(t/°\mathrm{C}) + c_2(t/°\mathrm{C})^2 + c_3(t/°\mathrm{C})^3 \tag{7}$$

and

$$\lambda_0/\mathrm{mW^{-1}\cdot m^{-1}\cdot K^{-1}} = d_0 + d_1(t/°\mathrm{C}) \tag{8}$$

The coefficients c_i were determined to be $c_0 = 6.965\ 39$, $c_1 = 4.952\ 12 \times 10^{-2}$, $c_3 = 5.911\ 57 \times 10^{-6}$, and $c_4 = 3.835\ 78 \times 10^{-6}$. The coefficients d_i correspond to the coefficients a_i in eq 6. Figure 8 shows that λ'' and λ_0 are nearly equal at −10 °C but begin to deviate as temperature increases. This further indicates that both the temperature and density have an obvious effect on the thermal conductivity.

Conclusion

An instrument contained two hot-wires was carefully developed and calibrated for measuring the thermal conductivity of fluids. Nitrogen was used to test the instrument. The thermal conductivity of gaseous CF_3I from −6.5 °C to 66.5 °C at pressures up to 1000 kPa with an uncertainty of less than 3% was obtained.

Acknowledgment

We are indebted to Dr. Nimitz, IKON Co., and Pacific Scientific for providing the CF_3I sample.

Literature Cited

Duan, Y. Y.; Zhu, M. S.; Han, L. Z. Experimental Vapor Pressure Data and a Vapor Pressure Equation for Trifluoroiodomethane (CF_3I). *Fluid Phase Equilib.* **1996**, *121*, 227−234.

Duan, Y. Y.; Zhu, M. S.; Shi, L.; Han, L. Z. Experimental PVT data and an equation of state for trifluoroiodomethane (CF_3I) in Gaseous Phase. *Fluid Phase Equilib.* **1997**, in press.

Healy, J. J.; De Groot, J. J.; Kestin, J. The Theory of the Transient Hot-wire Method for Measuring Thermal Conductivity. *Physica* **1976**, *82C*, 392−408.

Kestin, J.; Wakeham, W. A. A Contribution to the Theory of the Transient Hot-wire Technique for Thermal Conductivity Measurements. *Physica* **1978**, *92A*, 102−116.

Lankford, L.; Nimitz, J. A New Class of High-Performance, Environmentally Sound Refrigerants. *Proceedings of the Internation CFC and Halon Alternative Conference*, Washington DC, 1993; pp 141−149.

Menashe, J.; Wakeham, W. A. Absolute Measurements of the Thermal Conductivity of Liquids at Pressures up to 500 MPa. *Phys. Chem.* **1981**, *85*, 340−347.

Nieto de Castro, C. A.; Perkins, R. A.; Roder, H. M. Radiative Heat Transfer in Transient Hot-wire Measurements of Thermal Conductivity. *Int. J. Thermophys.* **1991**, *12*, 985−997.

Stephan, K.; Krauss, R.; Laesecke, A. Viscosity and Thermal Conductivity of Nitrogen for a Wide Range of Fluid States. *J. Phys. Chem. Ref. Data* **1987**, *16* (4), 993−1023.

Sun, L. Q.; Zhu, M. S.; Han, L. Z.; Lin, Z. Z. Thermal Conductivity of Gaseous Difluoromethane and Pentafluoroethane near the Saturation Line. *J. Chem. Eng. Data* **1997**, *42*, 179−182.

Zhao, X. Y.; Shi, L.; Zhu, M. S.; Han, L. Z. A New Generation of Long-Term Refrigerants as CFC-12 Alternatives. *Proceedings of the International CFC and Halon Alternatives Conference*, Washington, DC, 1995; pp 286−293.

Received for review February 2, 1997. Accepted May 16, 1997.[⊗] This work was supported by the State Education Commission of P.R. China.

JE9700378

[⊗] Abstract published in *Advance ACS Abstracts,* July 1, 1997.